Riddling of the Orbit in a High Dimensional Torus and Intermittent Energy Bursts in a Nonlinear Wave System

Kaifen He

CCAST (World Laboratory), Beijing, 100080 China

Institute of Low Energy Nuclear Physics, Beijing Normal University, Beijing, 100875 China

(Received 11 October 2004; published 25 January 2005)

The bifurcation scenario in a practically interesting nonlinear wave system is investigated by using a new scheme that is performed in a purely nonlinear wave framework with the Doppler effect taken into account. High-dimensional tori with three or four competing frequencies are observed. With variation of parameters a riddling of the orbit may occur intermittently due to tangency in certain dimensions, which temporarily spoils the toroidal topology and induces an energy burst where spatial coherence of the wave is lost.

DOI: 10.1103/PhysRevLett.94.034101 PACS numbers: 05.45.Jn

I. Introduction.—One of the mechanisms proposed for explaining the onset of turbulence is the Ruelle-Takens scenario. In this picture, chaos occurs when the third incommensurable frequency sets in that destroys the two-dimensional (2D) torus [1–3]. However, as pointed out in Ref. [4], experimental work served neither to confirm the theory nor to refute it. For example, in the drift-wave experiment this route is recognized to be responsible for the onset of weak turbulence [5], while in the nonlinear electronic oscillator circuit quasiperiodicity and chaos with three competing frequencies can appear in different parameter regimes [4], and in the Rayleigh-Bénard convection experiment nonchaotic states with four or five incommensurable frequencies are observed [6]. It is argued that spatial localization of the modes plays an important role in determining the route to chaos in an extended system [6].

Another relevant subject is intermittency [7–10], where the system switches back and forth intermittently between qualitatively different behaviors. For instance, in type-I intermittency the system is predominantly periodic with occasional "bursts" of chaotic behaviors, which, in mapping systems, are believed to arise from a tangent bifurcation. Intermittency is also observed in experiments, e.g., in Rayleigh-Bénard convection [11] and in plasmas [12]. The mechanism for intermittency in such spatially extended systems is still open.

With a driven-damped nonlinear wave system in previous works we revealed a mechanism for the critical transition to spatiotemporal chaos [13,14]. In the present Letter we focus on the regime before the transition. In this regime the wave is normally regular in space; however, with increasing driving force it becomes more and more erratic, and, in particular, when approaching the critical transition point bursts may occur intermittently in the wave energy. For understanding these phenomena we use a new method that allows us to pursue the bifurcation scenario entirely in a nonlinear wave framework; because of the wave propagation the Doppler effect has to be taken into account [15]. In Sect. II we show that a steady wave (SW) may lose its stability through a Hopf bifurcation; in Sect. III further bifurcations to high-dimensional tori with three or four competing frequencies are identified; in Sect. IV we show that with the variation of parameters a tangency may occur in certain dimensions, providing a possibility for the orbit to riddle through the toroidal(like) structure intermittently, which is responsible for the energy bursts. Finally, Sect. V is a discussion.

II. Hopf bifurcation from a steady wave.—The model equation is

$$\frac{\partial \phi}{\partial t} + a\frac{\partial^3 \phi}{\partial t \partial x^2} + c\frac{\partial \phi}{\partial x} + f\phi\frac{\partial \phi}{\partial x} = -\gamma\phi - \varepsilon \sin(x - \Omega t). \tag{1}$$

(Ω, ε) are two control parameters and a, c, f, γ are fixed the same as in Refs. [13,14]. With vanishing (Ω, ε) Eq. (1) is derived, respectively, as an alternative to the Korteweg–de Vries equation, in fluids to describe shallow water wave and in magnetized plasmas to describe drift wave [16]. In Refs. [13,14] a crisis-induced transition to turbulence in Eq. (1) is reported; for $\Omega = 0.65$ the critical transition point is $\varepsilon \approx 0.20$. In the present work we focus on the (Ω, ε) regime before the transition.

Let us start from an SW solution of Eq. (1) in the form of $\phi_0(x - \Omega t)$. Like any solitary wave, an SW has constant mode amplitudes and phases if observed in a reference frame moving in its group velocity; i.e., it is a fixed point in the Fourier space. For studying bifurcation behaviors from such a fixed point, we use a new scheme as follows [15]. When solving Eq. (1) with the pseudospectral method we expand $\phi(x, t) = \sum_{k=-N}^{N} \tilde{\phi}_k(t) e^{ikx}$; here complex $\tilde{\phi}_k(t) = \tilde{\phi}_{-k}(t)$ is governed by

$$(1 - ak^2)\frac{d\tilde{\phi}_k}{dt} + ick\tilde{\phi}_k + \frac{if}{2}\sum_{p+q=k} k\tilde{\phi}_p\tilde{\phi}_q + \gamma\tilde{\phi}_k - \frac{\varepsilon}{2}\delta_{1,k}[\sin\Omega t + i\cos\Omega t] = 0, \tag{2}$$

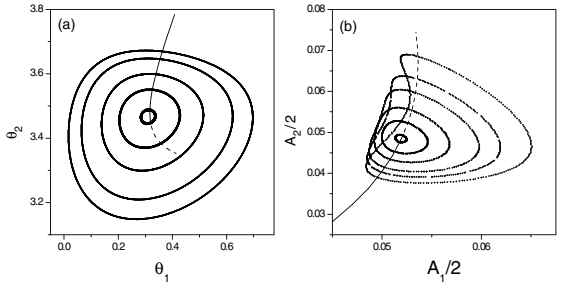

FIG. 1. Phase plot of (a) $\theta_2(\tau)$ vs $\theta_1(\tau)$ and (b) $A_2(\tau)/2$ vs $A_1(\tau)/2$ for $\Omega = 0.60$ and ε in the range of 0.06–0.07; the central line is obtained by solving the SW equation.

and hence in every time step we have information on $\{\tilde{\phi}_k(t)\}$. Rewriting $\phi(x, t) = \sum_{k=1}^{N} A_k(t)\cos[kx + \vartheta_k(t)]$, we have

$$A_k(t) = 2\sqrt{[\mathrm{Re}\,\tilde{\phi}_k(t)]^2 + [\mathrm{Im}\,\tilde{\phi}_k(t)]^2},$$
$$\tan\vartheta_k(t) = \mathrm{Im}\,\tilde{\phi}_k(t)/\mathrm{Re}\,\tilde{\phi}_k(t). \quad (3)$$

After its principal value is obtained, $\vartheta_k(t)$ can be determined within mod(2π) according to the signs of Re $\tilde{\phi}_k(t)$ and Im $\tilde{\phi}_k(t)$.

However, the $\{\vartheta_k(t)\}$ thus obtained are the phases in the (x, t) frame; we need to transform them to the frame $\xi = x - \Omega t$, $\tau = t$ where the SW is a fixed point. In this frame, if expanding $\phi(\xi, \tau) = \sum_{k=1}^{N} A_k(\tau)\cos[k\xi + \theta_k(\tau)]$, the following relation holds:

$$\theta_k(\tau) = \vartheta_k(\tau) + k\Omega t; \quad (4)$$

here phase shift $k\Omega t$ arises from the Doppler effect depending on wave number k. From the knowledge on $\{A_k(\tau), \theta_k(\tau)\}$ the bifurcation behaviors can be revealed. Here mod(2π) is taken in $\{\theta_k(\tau)\}$. When solving Eq. (1) grid numbers $N = 2^6$–2^9 are tested, and in the chosen regime the results agree with each other from the viewpoint of dynamics. For the present purpose $N = 2^6$ is used.

To test the method first we calculate $\{A_k(\tau), \theta_k(\tau)\}$ for a stable SW $\phi_0(\xi)$, e.g., $\Omega = 0.60$, $\varepsilon < \sim 0.065$; indeed, $\{A_k(\tau), \theta_k(\tau)\}$ tend to constant values which are in agreement with that obtained by solving the SW equation $\partial\phi_0/\partial\tau = 0$. At $\varepsilon \sim 0.065$ the SW loses its stability. In Figs. 1(a) and 1(b) we plot $\theta_2(\tau)$ vs $\theta_1(\tau)$ and $A_2(\tau)$ vs $A_1(\tau)$ for several ε values in the range 0.065–0.07; here and in the following transient states have been omitted. In both plots one can see a set of circles with a line penetrating through the center. The circles are obtained by the present procedure; the line shows the SW solutions obtained from $\partial\phi_0/\partial\tau = 0$. The dashed parts of the lines indicate that the corresponding SW's are unstable; it is from there the limit cycles are bifurcated, obviously due to a Hopf instability.

III. Further bifurcations to high-dimensional tori.—In the following we fix $\Omega = 0.65$ and vary ε to study the bifurcations further from the limit cycles. Figure 2 shows

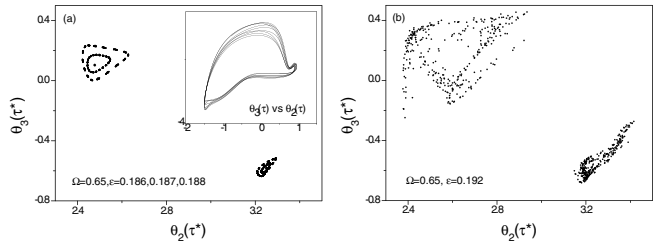

FIG. 2. Poincaré section $\theta_3(\tau^*)$ vs $\theta_2(\tau^*)$ cut at $\theta_1(\tau) = 1, \pm\pi$ for (a) $\varepsilon = 0.186, 0.187, 0.188$ and (b) $\varepsilon = 0.192$, $\Omega = 0.65$; the inset is phase plot $\theta_3(\tau)$ vs $\theta_2(\tau)$ for $\varepsilon = 0.188$.

Poincaré sections $\theta_3(\tau^*)$ vs $\theta_2(\tau^*)$; here τ^* denotes the moments when $\theta_1(\tau) = 0$ or $\pm\pi$. For $\varepsilon = 0.186$ the orbit is a limit cycle, and in Fig. 2(a) it manifests as two isolated points. Surrounding the two points one can find nested circles obtained for $\varepsilon = 0.187$ and 0.188, respectively, indicating that the limit cycle has bifurcated into 2D torus (in the following we see that in these cases the third frequency already sets in; since it is very weak, the Poincaré sections still look like smooth circles). The inset of Fig. 2(a) depicts $\theta_3(\tau)$ vs $\theta_2(\tau)$ for $\varepsilon = 0.188$ without taking the Poincaré section; the orbit displays as a wide cyclic band. With an increase of ε the circles in Fig. 2(a) gradually become larger and even the section points may become somewhat scattered. Figure 2(b) is an example of $\theta_3(\tau^*)$ vs $\theta_2(\tau^*)$ for $\varepsilon = 0.192$, where one can find two patches locating about at the places where the nested circles used to be in Fig. 2(a). Compared with 2(a) the patch sizes in 2(b) are larger and the points are a little scattered, indicating that the 2D torus becomes ''fat'' and further bifurcation(s) have occurred. In other Poincaré sections in this regime, $\theta_k(\tau^*)$ vs $\theta_{k'}(\tau^*)$ or $A_k(\tau^*)$ vs $A_{k'}(\tau^*)$, one can also find two well-separated patches as

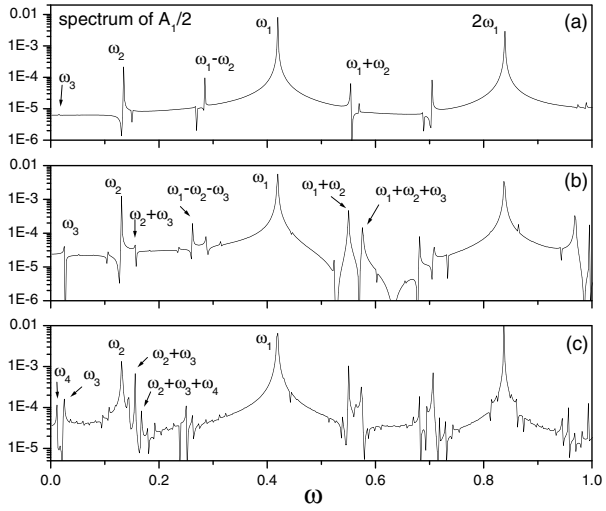

FIG. 3. Spectrum of $A_1(\tau)/2$ for (a) $\varepsilon = 0.1865$, (b) $\varepsilon = 0.188$, and (c) $\varepsilon = 0.189$, $\Omega = 0.65$.

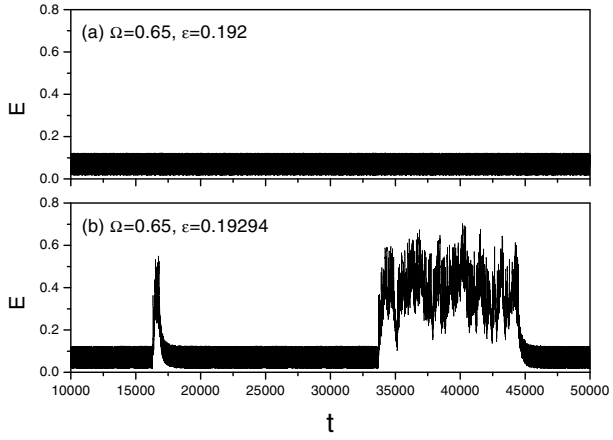

FIG. 4. Evolution of wave energy $E(t)$ for $\Omega = 0.65$ with (a) $\varepsilon = 0.192$ and (b) $\varepsilon = 0.192\,94$.

in Fig. 2, suggesting that the topology still has a skeleton of the 2D torus; it is something like a "coarse doughnut."

By calculating the Fourier spectrum, e.g., of $A_k(\tau)$, one can clearly see how a limit cycle bifurcates to high-dimensional tori. In the spectrum of a limit cycle, e.g., $\varepsilon = 0.186$, there is only one independent frequency at $\omega_1 \approx 0.42$. With increasing ε a new frequency appears. Figure 3 shows the spectrum of $A_{k=1}(\tau)$: Figure 3(a) For $\varepsilon = 0.1865$, one can find two incommensurable frequencies, $\omega_1 \approx 0.42$, $\omega_2 \approx 0.13$, as well as their beat frequencies; it is even noticed that the third frequency, ω_3, starts to show up at a very low frequency. Figure 3(b) For $\varepsilon = 0.188$, evidently the spectrum is composed of three competing frequencies ω_1, ω_2, and ω_3. When $\varepsilon = 0.189$ in Fig. 3(c), one can identify a new frequency ω_4 and its beat frequencies with three other ones. For ε up to about 0.191 the spectra are still isolated lines, and the attractors are of higher dimensional toroidal(like) topology.

When ε is increased to $\sim$0.192, detailed identification becomes difficult. Nevertheless, as one has seen in Fig. 2(b), the attractor still has a skeleton of the 2D torus. With further increasing ε, however, a new phenomenon sets in, as will be described in the next section.

IV. Riddling of orbit and intermittent energy burst.— Figure 4 shows evolution of the wave energy, $E(t) = \frac{1}{2\pi} \times \int_0^{2\pi} \frac{1}{2}[\phi^2 - a\phi_x^2]dx$, for 4(a) $\varepsilon = 0.192$ and 4(b) $\varepsilon = 0.192\,94$. A remarkable phenomenon is that in 4(b) $E(t)$ bursts up occasionally in contrast to smooth oscillations in 4(a).

To understand this new phenomenon, let us plot the Poincaré section $A_{k\neq 1}(\tau^*)$ vs $A_1(\tau^*)$ at $\theta_1(\tau^*) = 0, \pm\pi$. With variation of $\{\Omega, \epsilon\}$ one can also observe the bifurcation sequence of fixed point → limit cycle → 2D torus → high-dimensional tori(like). With the doughnut becoming increasingly fat and coarse, the section patches are gradually enlarged and the section points become a little scattered. If there is no burst, like in the case of $\varepsilon = 0.192$, two patches of the Poincaré section are clearly separated in any dimension, similar to Fig. 2(b). When an intermittent burst occurs, however, the situation is different. Figure 5 shows $A_k(\tau^*)$ vs $A_1(\tau^*)$ for $\varepsilon = 0.192\,94$, in the periods of 5(a) $\tau = 15\,000$–$20\,000$, 5(b) $\tau = 20\,000$–$25\,000$, and 5(c) and 5(d) $\tau = 35\,000$–$45\,000$, with $k = 3$ in 5(a)–5(c) and $k = 2$ in 5(d), respectively. In the plots, crosses or bullets denote the section points cut at $\theta_1 = 0/\pm\pi$. Figure 5(b) corresponds to a time period when $E(t)$ oscillates smoothly; one can see that the two patches almost get touched; that is, a tangency occurs. Figure 5(a) is in a period when $E(t)$ experiences a narrow burst as well as smooth oscillations; in this case there are still two patches concentrated with crosses and bullets, respectively; however, a few cross or bullet points have invaded (or riddled) into the region bullets or cross points used to occupy. If examining the data carefully one finds that the onset of the burst is just related to the occurrence of the riddling. Finally, Fig. 5(c) corresponds to a time interval when $E(t)$ is completely in a bursty period; one can see that the section points become extremely scattered, and the bullets and crosses are mingled with each other. Obviously in this

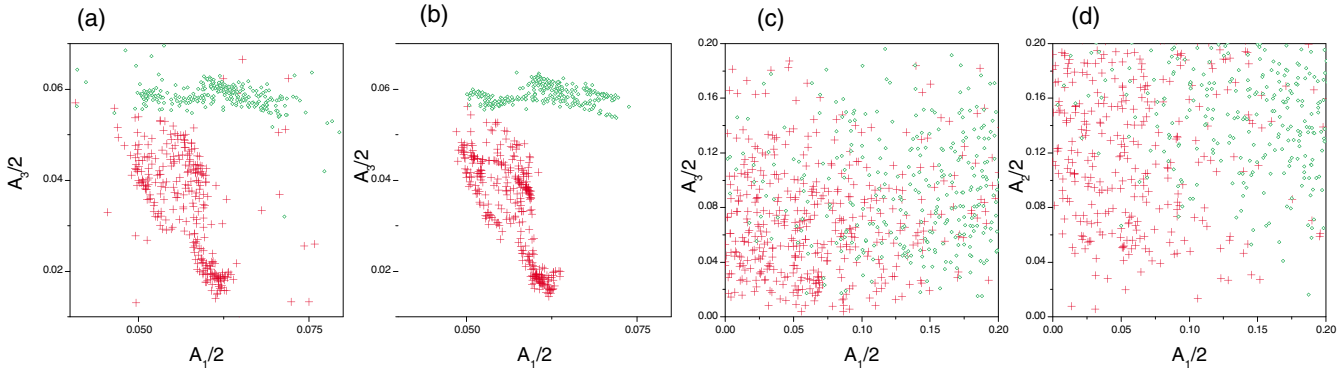

FIG. 5 (color online). Poincaré section $A_k(\tau^*)/2$ vs $A_1(\tau^*)/2$ for $\Omega = 0.65$ and $\varepsilon = 0.192\,94$ in the period of (a) 15 000–20 000, (b) 20 000–25 000, and (c),(d) 35 000–45 000; in (a)–(c) $k = 3$, and in (d) $k = 2$; crosses and bullets denote the section points cut at $\theta_1(\tau) = 0, \pm\pi$, respectively.

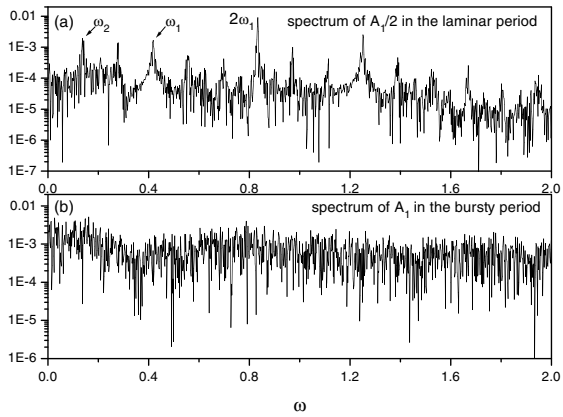

FIG. 6. Spectrum of $A_1(\tau)/2$ for $\Omega = 0.65$, $\varepsilon = 0.192\,94$ in (a) a smooth oscillation period, and (b) a bursty period.

case no toroidal topology is sustained at all. Our investigation shows that the tangency and riddling occur first between two amplitudes [e.g., A_3 vs A_1 as in Figs. 5(a)–5(c)], then the riddling spreads to other ones. In Fig. 5(d) we plot $A_2(\tau^*)$ vs $A_1(\tau^*)$ for the same period of 5(c), where cross or bullet points are also very scattered, despite the fact that in the smooth oscillating periods the two section patches of $A_2(\tau^*)$ vs $A_1(\tau^*)$ are far apart from each other. The above results convince us that the bursts in wave energy are induced by orbit riddlings. The picture we draw from the above phenomena is as follows: as the coarse doughnut becomes ''fatter'' the central hole of it vanishes in certain dimensions; that is, a tangency occurs. The orbit then has a possibility to riddle through the vanished hole and can be wandering in a much larger phase space. As a result, the toroidal topology is spoiled, inducing the mode amplitudes and hence the wave energy to burst up chaotically.

Figure 6 is the spectrum of $A_1(\tau)$ for $\varepsilon = 0.192\,94$: 6(a) A smooth oscillation period, in which one can identify two major competing frequencies characteristic of the ''skeleton'' of 2D torus, in contrast to the bursty period in 6(b), where no any characteristic frequency can be seen.

We also plotted space-time patterns for $\varepsilon = 0.192\,94$; the spatial coherence is temporarily lost in the bursty periods.

V. Conclusion and discussion.—We have shown in a nonlinear wave system that a steady wave may lose its stability through a Hopf bifurcation. Further bifurcations to higher dimensional tori with up to four competing frequencies have also been identified; this observation is consistent with the experiments in fluids and plasmas [3,4,6]. With increasing driving force a tangency occurs in certain dimensions; in this case an orbit riddling may happen intermittently. The orbit riddling temporarily destroys the toroidal topology, which is responsible for the intermittent burst of the wave energy where the spatial coherence is lost. Since they occur in the regime before the transition to a strong turbulent state, these phenomena are presumably related to so-called weak turbulence. Compared to bursts in strong turbulence [14], the bursts in the present case show different features, and their mechanisms are completely different.

In a model of three drift-wave interaction [17] chaos occurs when the third frequency appears, which supports the prediction of the Ruelle-Takens scenario. In our extended system, however, the toroidal topology remains even when three or four competing frequencies are present. Probably spatial localization plays a role in this respect. Further investigations are needed to confirm this conjecture.

Our investigation is done by directly solving the nonlinear wave equation without further restriction for the wave solutions except for the periodicity, so we are convinced that the revealed phenomena reflect what happens in the nonlinear wave. It is expected that the method can be applied to other spatially extended systems for theoretical and experimental analyses for the nonlinear dynamics.

This work is supported by the special funds for Major State Basic Research of China and by NSFC No. 10475009 and No. 10335010.

[1] A. J. Lichtenberg and M. A. Lieberman, *Regular and Stochastic Motion* (Springer-Verlag, New York, 1983).
[2] R. C. Hilborn, *Chaos and Nonlinear Dynamics: An Introduction for Scientists and Engineers* (Oxford University Press, Inc., New York, 1994).
[3] P. G. Drazin, *Nonlinear Systems* (Cambridge University Press, Cambridge, 1992), Chap. 8.
[4] A. Cumming and P. S. Linsay, Phys. Rev. Lett. **60**, 2719 (1988).
[5] T. Klinger, A. Latten, A. Piel, G. Bonhomme, T. Pierre, and T. Dudok de Wit, Phys. Rev. Lett. **79**, 3913 (1997).
[6] R. W. Walden, P. Kolodner, A. Passner, and C. M. Surko, Phys. Rev. Lett. **53**, 242 (1984).
[7] P. Manneville and Y. Pomeau, Phys. Lett. **75A**, 1 (1979),Y. Pomeau and P. Manneville, Commun. Math. Phys. **74**, 189 (1980).
[8] E. Ott, *Chaos in Dynamical Systems* (Cambridge University Press, Cambridge, 1993), p. 272.
[9] N. Platt, E. A. Spiegel, and C. Tresser, Phys. Rev. Lett. **70**, 279 (1993).
[10] P. W. Hammer, N. Platt, S. M. Hammel, J. F. Heagy, and B. D. Lee, Phys. Rev. Lett. **73**, 1095 (1994).
[11] P. Berge, M. Dubois, M. Manneville, and Y. Pomeau, J. Phys. Lett. **41**, L341 (1980).
[12] P. Y. Cheung, S. Donovan, and A. Y. Wong, Phys. Rev. Lett. **61**, 1360 (1988).
[13] Kaifen He, Phys. Rev. Lett. **80**, 696 (1998); **84**, 3290 (2000); Phys. Rev. E **63**, 016218 (2001).
[14] Kaifen He and A. C.-L. Chian, Phys. Rev. Lett. **91**, 034102 (2003); Phys. Rev. E **69**, 026207 (2004).
[15] Kaifen He, Chin. Phys. Lett. **21**, 439 (2004).
[16] Kaifen He, Int. J. Mod. Phys. B **18**, 1805 (2004), and references therein.
[17] D. Biskamp and Kaifen He, Phys. Fluids **28**, 2172 (1985).